Research Square

Preprints are preliminary reports that have not undergone peer review.
They should not be considered conclusive, used to inform clinical practice,
or referenced by the media as validated information.

Photoinitiated Cationic Copolymerization of Cyclohexene Oxide and Cyclopentene Oxide: Monomer Reactivity Ratios and the Composition Dependence of the Glass Transition Temperature

Ideisan Ibrahim Abu-Abdoun

ideisan@gmail.com

University of Petra Faculty of Arts and Sciences https://orcid.org/0000-0003-4230-462X

Abdelmnim M. Al Tweiq

Leen N. Ali

Research Article

Keywords: cationic photopolymerization, cyclohexene oxide, cyclopentene oxide, reactivity ratios, glass transition temperature, cycloaliphatic epoxides

Posted Date: November 11th, 2026

DOI: https://doi.org/10.21203/rs.3.rs-11503372/v1

License: This work is licensed under a Creative Commons Attribution 4.0 International License.
Read Full License

Photoinitiated Cationic Copolymerization of Cyclohexene Oxide and Cyclopentene Oxide: Monomer Reactivity Ratios and the Composition Dependence of the Glass Transition Temperature

Ideisan I. Abu-Abdoun*, Abdelmnim M. Al Tweiq and Leen N. Ali

Department of Chemistry, University of Petra, Amman, Jordan

*Correspondence to: I. I. Abu-Abdoun, e-mail: ideisan.abuabdoun@uop.edu.jo; alternative e-mail: ideisan@gmail.com; ORCID: 0000-0003-4230-462X

Abstract

The photoinitiated cationic copolymerization of cyclohexene oxide (CHO) and cyclopentene oxide (CPO) was investigated at 25 °C using (4-phenylthiophenyl)diphenylsulfonium hexafluorophosphate (PTPDS PF_6^-) as the photoinitiator and 366 nm irradiation. Dilatometric measurements on the homopolymerizations showed that CHO polymerizes approximately 1.8 times faster than CPO and with a shorter induction period. Copolymer compositions, determined by ^{13}C NMR spectroscopy for ten feed compositions at low conversion, were consistently richer in CHO than the corresponding feeds. The Kelen–Tüdős method gave monomer reactivity ratios of $r_{CHO} = 2.45$ and $r_{CPO} = 0.69$, and nonlinear least-squares fitting of the Mayo–Lewis equation gave $r_{CHO} = 2.65 \pm 0.25$ and $r_{CPO} = 0.77 \pm 0.08$ ($r_{CHO}r_{CPO} \approx 2.0$). The copolymers are therefore statistical, with preferential incorporation of CHO and a modest tendency towards CHO homosequences. Each copolymer exhibited a single glass transition temperature (T_g), which decreased from 337.3 K (64.2 °C) for poly(CHO) to 254.9 K (−18.3 °C) for poly(CPO). The T_g–composition curve showed a pronounced negative deviation from both linear additivity and the Fox equation, reaching −18.5 K at only 5.4 mol% CPO, whereas the number-average molar mass (16–20 kg mol^{-1}) was essentially independent of composition. This behaviour is attributed to the increased segmental mobility that results when isolated cyclopentane units separate neighbouring cyclohexane rings along the polyether backbone, an

interpretation supported by the contrasting ^{13}C NMR line shapes of the two homopolymers. The data provide composition–property relationships for the design of cationically UV-cured coatings and adhesives based on cycloaliphatic epoxides.

Keywords: cationic photopolymerization; cyclohexene oxide; cyclopentene oxide; reactivity ratios; glass transition temperature; cycloaliphatic epoxides

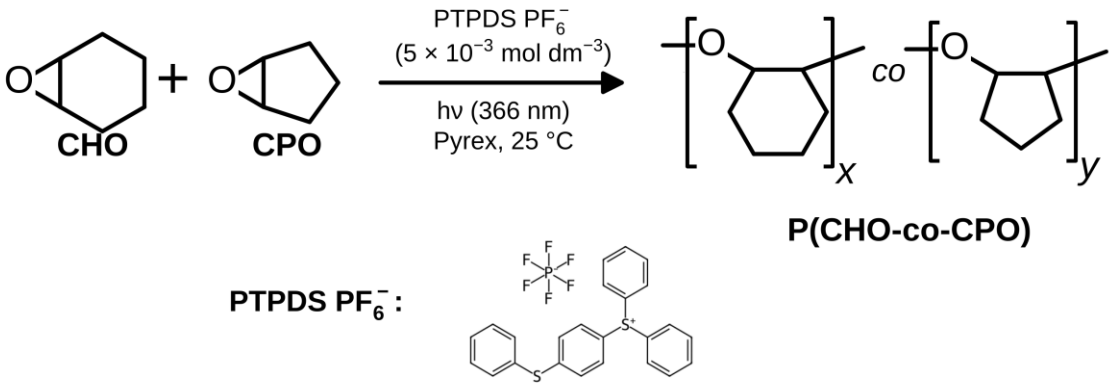
1. Introduction

Photoinitiated cationic polymerization of epoxides is the basis of a large family of UV-curable coatings, inks, adhesives and encapsulants. Since the introduction of diaryliodonium and triarylsulfonium salts as efficient photoacid generators [1–3], cycloaliphatic epoxides have become the preferred monomers for these applications because their ring strain and the basicity of the oxirane oxygen give high rates of ring-opening polymerization, low shrinkage, good adhesion and insensitivity to oxygen inhibition [4, 5]. Cyclohexene oxide (CHO) is the simplest cycloaliphatic epoxide and is widely used as a model monomer for mechanistic and kinetic studies, whereas its lower homologue, cyclopentene oxide (CPO), has received considerably less attention.

Commercial formulations are usually mixtures of several epoxide monomers, and their cured properties depend on how the comonomers are distributed along the polymer chains. Quantitative information on comonomer reactivity in cationic ring-opening copolymerization is, however, much scarcer than for radical copolymerization. The reactivity ratios that describe the composition and sequence distribution of a copolymer can be obtained from low-conversion composition data with the terminal (Mayo–Lewis) model [6], using either linearized methods such as those of Fineman–Ross [7] and Kelen–Tüdős [8] or, preferably, nonlinear least-squares fitting, which avoids the statistical distortions introduced by linearization [9, 10].

The glass transition temperature (T_g) of a random copolymer is commonly estimated from the homopolymer values with additive relationships such as the Fox [11] and Gordon–Taylor [12] equations. Significant deviations from these relationships indicate that the T_g also depends on the sequence distribution, that is, on the local environment of each repeat unit, as formalized in the dyad models of Johnston [13] and Barton [14].

We have previously studied the photoinitiated polymerization of cyclohexene oxide with phosphonium and arsonium salts [15] and with dirhenium decacarbonyl [16]. Here we report the photoinitiated cationic copolymerization of CHO and CPO with the sulfonium salt PTPDS PF_6^- [17] (Scheme 1). The homopolymerization rates were compared by dilatometry, the copolymer compositions were determined by ^{13}C NMR spectroscopy over the full feed range, and the reactivity ratios were evaluated by linear and nonlinear methods. The composition dependence of T_g and of the number-average molar mass was then measured to establish composition–property relationships relevant to cycloaliphatic epoxide formulations. The measurements were made with the classical techniques described in Section 2. Here they are evaluated with current data-analysis methods, namely nonlinear least-squares estimation of the reactivity ratios with joint confidence regions, as now recommended by IUPAC [10], and a sequence-distribution analysis of the glass transition, which together give a more reliable and more detailed picture of this copolymerization than linearized treatments.



Scheme 1 Photoinitiated cationic copolymerization of cyclohexene oxide (CHO) and cyclopentene oxide (CPO) with (4-phenylthiophenyl)diphenylsulfonium hexafluorophosphate (PTPDS PF_6^-). Both repeat units have the *trans*-1,2-configuration that results from S_N2-type ring opening of the oxiranium ion

2. Experimental

2.1. Materials

Commercial cyclohexene oxide (CHO) and cyclopentene oxide (CPO) were purified by drying over freshly ground calcium hydride followed by fractional distillation. Densities of 0.967 g cm^{-3} (CHO) and 0.964 g cm^{-3} (CPO) at 25 °C and molar masses of 98.14 and 84.12 g mol^{-1} were used to convert volumes into moles. The photoinitiator (4-phenylthiophenyl)diphenylsulfonium hexafluorophosphate (PTPDS PF_6^-) was prepared according to the procedure of Smith [17] and recrystallized before use. $CDCl_3$ (99.8 atom% D, containing TMS) was used as received.

2.2. Dilatometric homopolymerization

Homopolymerization rates were measured by dilatometry in bulk. PTPDS PF_6^- was dissolved in the neat monomer at a concentration of 5×10^{-3} mol dm^{-3}. The solution was transferred into a Pyrex dilatometer, degassed by three freeze–pump–thaw cycles and thermostatted at 25.0 ± 0.1 °C in a water bath. Irradiations were carried out in a Rayonet merry-go-round photochemical reactor (model RPR-100, Southern New England Ultraviolet Co.), in

which the samples are held in a merry-go-round holder that is rotated continuously by a motor inside the reactor barrel. The holder is surrounded by 16 lamp tubes emitting at 366 nm, at a distance of 5 cm from the samples, as described previously [16]. The fall in meniscus height (Δh) was recorded as a function of irradiation time. Pyrex was used throughout to exclude wavelengths below about 300 nm. The rate of polymerization was obtained from the slope of the linear, post-induction part of the contraction curve as

$$R_p = (dh/dt)A / (V_0 \Delta V_m) \quad (1)$$

where A is the cross-sectional area of the capillary, V_0 the initial volume of the solution and ΔV_m the molar volume contraction on polymerization, calculated from the monomer and polymer densities.

2.3. Copolymerization

Ten comonomer mixtures with CHO/CPO volume ratios from 95/5 to 10/90 were prepared with a total volume of 5 cm^3. The corresponding molar feed compositions are listed in Table 1. PTPDS PF_6^- (5×10^{-3} mol dm^{-3}) was dissolved in each mixture, and the solutions were degassed in Pyrex tubes, sealed and irradiated at 366 nm and 25 °C in the same merry-go-round photoreactor, whose continuous rotation ensured equal irradiation of all samples. Irradiation was stopped at low conversion (below 10%), so that the feed composition could be regarded as constant during copolymerization. The copolymers were precipitated in methanol, purified by redissolution in dichloromethane and reprecipitation, and dried under vacuum at 40 °C to constant weight. Poly(CHO) and poly(CPO) were prepared in the same way from the pure monomers.

2.4. Characterization

^{13}C NMR spectra were recorded at 25.2 MHz on a Varian XL-100 spectrometer from $CDCl_3$ solutions in 5 mm tubes at the probe temperature, with the deuterium signal of $CDCl_3$ as the lock and TMS as the internal reference ($\delta = 0$). Spectra were acquired over a 5000 Hz

sweep width with broadband (noise-modulated) ^{1}H decoupling and about 14 000 transients; the sample spinning rate was 35 Hz. Copolymer compositions were calculated from the relative integrated intensities of the resolved resonances of the CHO and CPO units.

Glass transition temperatures were determined by differential scanning calorimetry (DSC) under nitrogen, using the heating rate and procedure described previously [18]. T_g was taken as the midpoint of the heat-capacity step in the second heating scan, after a first scan to erase the thermal history. Number-average molar masses (M_n) were determined by gel permeation chromatography (GPC) at 25 °C, with tetrahydrofuran (THF) as the eluent at a flow rate of 1 cm^3 min^{-1}, using calibration with narrow-dispersity polystyrene standards.

2.5. Evaluation of reactivity ratios

With CHO as monomer 1 and CPO as monomer 2, the instantaneous copolymer composition is given by the Mayo–Lewis equation [6]:

$$F_1 = (r_1 f_1^2 + f_1 f_2) / (r_1 f_1^2 + 2 f_1 f_2 + r_2 f_2^2) \quad (2)$$

where f_i and F_i are the mole fractions of monomer i in the feed and in the copolymer, respectively. For the Kelen–Tüdős (K–T) analysis [8], $x = [M_1]/[M_2]$ in the feed, $y = d[M_1]/d[M_2]$ in the copolymer, $G = x(y - 1)/y$ and $F = x^2/y$, and the data are plotted according to

$$\eta = (r_1 + r_2/\alpha)\xi - r_2/\alpha \quad (3)$$

where $\eta = G/(\alpha + F)$, $\xi = F/(\alpha + F)$ and $\alpha = (F_{min}F_{max})^{1/2}$. The intercepts of the line at $\xi = 1$ and $\xi = 0$ give r_1 and $-r_2/\alpha$, respectively. In addition, r_1 and r_2 were obtained by nonlinear least-squares (NLLS) fitting of Eq. (2) to the F_1–f_1 data (Levenberg–Marquardt algorithm), and the 95% joint confidence region (JCR) was calculated from the residual sum of squares using the F-distribution [9, 10].

3. Results and discussion

3.1. Homopolymerization of CHO and CPO

Fig. 1 compares the dilatometric contraction curves for the homopolymerization of CHO and CPO under identical conditions. After an induction period, both monomers polymerized at a constant rate. The induction period was markedly shorter for CHO (≈5 min) than for CPO (≈11 min), and the rate of contraction was about twice as high (0.353 vs 0.167 cm min^{-1}). After correction for the different molar volume contractions of the two monomers (Eq. (1)), CHO polymerized 1.79 times faster than CPO.

The lower reactivity of CPO is consistent with the thermodynamics and stereochemistry of ring opening. Propagation proceeds by S_N2-type attack of monomer on the tertiary oxonium (oxiranium) chain end, with inversion at the attacked carbon, and therefore yields *trans*-1,2-disubstituted rings. A *trans*-1,2-disubstituted cyclohexane ring can adopt a strain-free diequatorial chair conformation, whereas the corresponding cyclopentane unit retains substantial torsional strain. Ring opening of CHO thus releases more strain than ring opening of CPO. CHO would therefore be expected to be incorporated preferentially in the copolymerization.

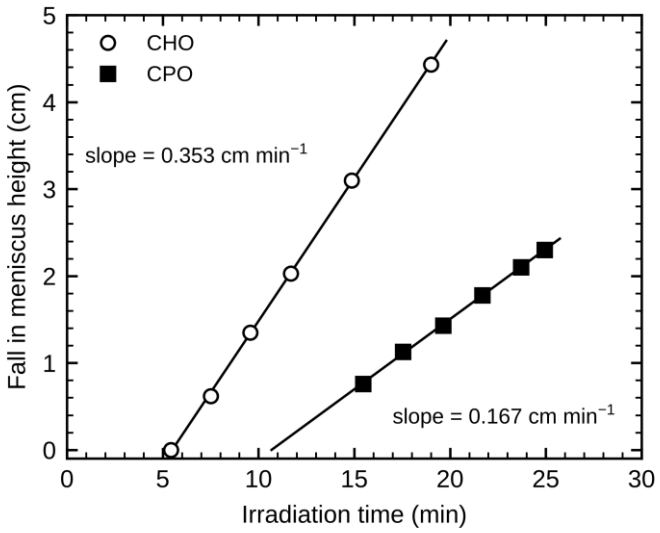


Fig. 1 Dilatometric contraction curves for the photoinitiated cationic homopolymerization of CHO (○) and CPO (■). [PTPDS PF_6^-] = 5 × 10^{-3} mol dm^{-3}; λ = 366 nm; Pyrex; 25 °C. Lines are least-squares fits to the linear (post-induction) region

3.2. Copolymer composition and reactivity ratios

The feed and copolymer compositions are listed in Table 1 and plotted in Fig. 2. Throughout the composition range the copolymer contained less CPO than the feed, so all data points lie below the azeotropic line. This confirms the preferential incorporation of CHO anticipated from the homopolymerization rates.

Table 1. Feed and copolymer compositions for the photoinitiated cationic copolymerization of CHO (M_1) and CPO (M_2).

Feed volume (cm^3)[a]		Feed (mol)		Feed mole fraction		Copolymer mole fraction[b]	
CHO	CPO	CHO	CPO	f_{CHO}	f_{CPO}	F_{CHO}	F_{CPO}
4.75	0.25	0.0468	0.0029	0.9422	0.0577	0.970	0.030
4.50	0.50	0.0443	0.0057	0.8855	0.1145	0.946	0.054
4.00	1.00	0.0394	0.01146	0.7743	0.2257	0.897	0.103
3.50	1.50	0.0345	0.01719	0.6666	0.3334	0.806	0.194
3.00	2.00	0.02954	0.02292	0.5631	0.4369	0.730	0.270
2.50	2.50	0.02461	0.02865	0.4619	0.5381	0.648	0.352
2.00	3.00	0.01969	0.03438	0.3642	0.6358	0.537	0.463
1.50	3.50	0.01477	0.04011	0.2691	0.7309	0.375	0.625
1.00	4.00	0.00985	0.04584	0.1769	0.8231	0.231	0.769

Feed volume (cm^3)[a]		Feed (mol)		Feed mole fraction		Copolymer mole fraction[b]	
CHO	CPO	CHO	CPO	f_{CHO}	f_{CPO}	F_{CHO}	F_{CPO}
0.50	4.50	0.00492	0.05157	0.0871	0.9129	0.148	0.852

[a] Total volume 5 cm^3; CHO/CPO volume ratios from 95/5 to 10/90. [b] Determined by ^{13}C NMR spectroscopy at low conversion.

The Kelen–Tüdős variables are listed in Table 2 and the K–T plot is shown in Fig. 3a. The nine copolymers from 90/10 to 10/90 ($\alpha = 0.423$) gave a good straight line ($R^2 = 0.967$), from which $r_{CHO} = 2.45$ and $r_{CPO} = 0.69$. The 95/5 copolymer was omitted from the linearized analysis because of its high leverage in the K–T plot, but it was included in the nonlinear fit. NLLS fitting of Eq. (2) to all ten data points, the procedure recommended by IUPAC [10], gave $r_{CHO} = 2.65 \pm 0.25$ and $r_{CPO} = 0.77 \pm 0.08$ (Table 3). The two methods agree: the K–T estimate lies close to the NLLS optimum and well inside the 95% JCR (Fig. 3b), and the Mayo–Lewis curves calculated from both parameter sets reproduce the experimental compositions closely (Fig. 2; root-mean-square residual in $F_{CHO} = 0.016$). The NLLS values are adopted in the following discussion.

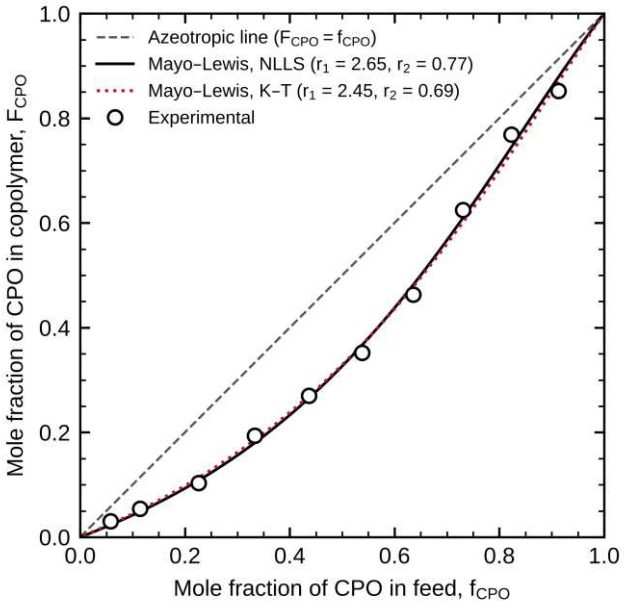


Fig. 2 Copolymer composition curve for the CHO/CPO system: mole fraction of CPO in the copolymer (F_{CPO}) versus that in the feed (f_{CPO}). Symbols: experimental data (Table 1). Curves: Mayo–Lewis

178 equation with the NLLS (solid) and Kelen–Tüdős (dotted) reactivity ratios. The dashed line marks F_{CPO}
179 = f_{CPO}

180 **Table 2.** Kelen–Tüdős variables for the CHO (M_1)/CPO (M_2) copolymerization (α = 0.423).

CHO/CPO (v/v)	*x*	*y*	*F*	*G*	ξ	η
90/10	7.734	17.519	3.414	7.292	0.890	1.900
80/20	3.431	8.709	1.351	3.037	0.762	1.711
70/30	1.999	4.155	0.962	1.518	0.695	1.096
60/40	1.289	2.704	0.614	0.812	0.592	0.783
50/50	0.858	1.841	0.400	0.392	0.486	0.476
40/60	0.573	1.160	0.283	0.079	0.401	0.112
30/70	0.368	0.600	0.226	-0.245	0.348	-0.378
20/80	0.215	0.300	0.154	-0.501	0.267	-0.868
10/90	0.095	0.174	0.052	-0.454	0.110	-0.955

181 $x = [M_1]/[M_2]$ (feed); $y = d[M_1]/d[M_2]$ (copolymer); $G = x(y - 1)/y$; $F = x^2/y$; $\eta = G/(\alpha + F)$; $\xi = F/(\alpha + F)$.

182 **Table 3.** Monomer reactivity ratios for the photoinitiated cationic copolymerization of CHO (M_1) and
183 CPO (M_2).

Method	Data points	r_1 (CHO)	r_2 (CPO)	r_1r_2
Kelen–Tüdős	9[a]	2.45	0.69	1.69
NLLS, Mayo–Lewis eq.	10	2.65 ± 0.25[b]	0.77 ± 0.08[b]	2.04
95% JCR (NLLS)	10	2.04–3.57	0.58–1.06	1.20–3.72

184 [a] 90/10 to 10/90 feeds; α = 0.423. [b] Asymptotic standard errors.

185 The reactivity ratios show that the CHO-terminated (oxonium) chain end adds CHO
186 about 2.5 times faster than CPO, whereas the CPO-terminated chain end adds CHO slightly
187 faster than CPO ($1/r_{CPO} \approx 1.3–1.5$). The product $r_{CHO}r_{CPO}$ is 2.04 (NLLS; 1.69 by K–T), and
188 the entire 95% JCR lies above the hyperbola $r_1r_2 = 1$ (minimum value 1.2), so that the deviation
189 from ideal random copolymerization is statistically significant. The copolymers are therefore
190 statistical rather than alternating or blocky, with a modest tendency towards CHO
191 homosequences.

192 With the NLLS reactivity ratios, the terminal model [19] predicts number-average
193 sequence lengths of 1.05 CPO units and about 44 CHO units at $f_{CPO} = 0.058$, 1.9 CPO units and
194 3.3 CHO units at $f_{CPO} = 0.54$, and 9.1 CPO units and 1.25 CHO units at $f_{CPO} = 0.91$. Thus, in

CHO-rich copolymers the CPO units are almost exclusively isolated between CHO units. This point is important for the discussion of the glass transition below.

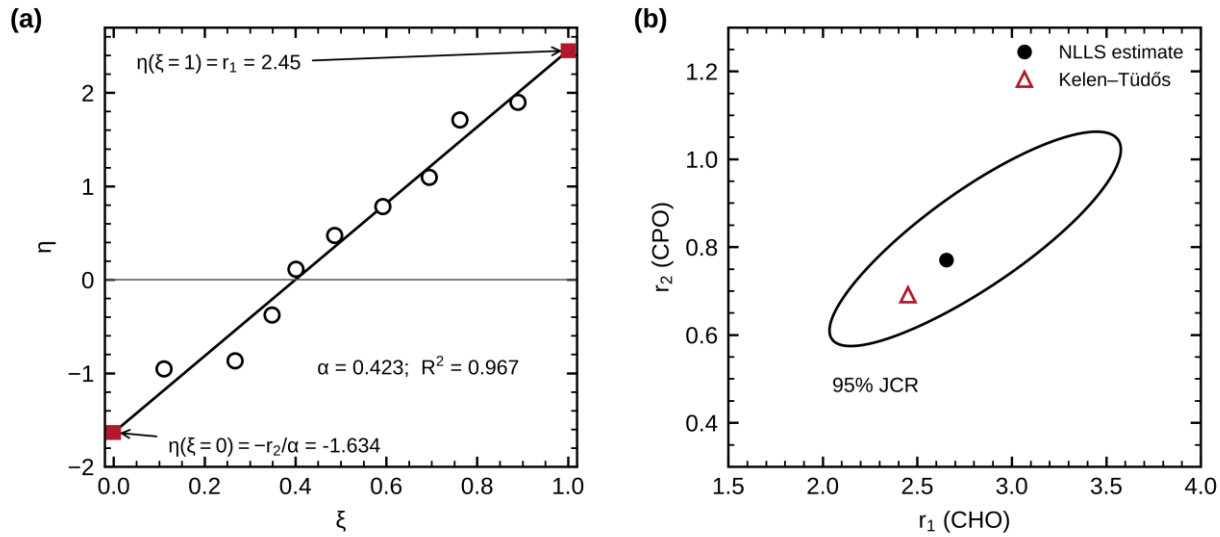


Fig. 3 (a) Kelen–Tüdős plot for the copolymerization of CHO (M_1) and CPO (M_2) (data from Table 2); the intercepts at $\xi = 1$ and $\xi = 0$ give r_1 and $-r_2/\alpha$, respectively. (b) 95% joint confidence region for r_1 and r_2 obtained by NLLS fitting of the Mayo–Lewis equation, with the NLLS (●) and Kelen–Tüdős (△) estimates

3.3. Glass transition temperature and molar mass

All copolymers showed a single glass transition, which lay between those of the two homopolymers (Table 4, Fig. 4). This, together with the NMR compositions, confirms that copolymers rather than blends of the homopolymers were formed. The T_g decreased from 337.3 K for poly(CHO) to 254.9 K for poly(CPO), a difference of 82.4 K. Over the whole composition range the number-average molar mass remained between 16 and 20 kg mol^{-1}, without any systematic trend (Table 4). The variation of T_g with composition therefore cannot be attributed to differences in chain length.

Table 4. Glass transition temperatures and number-average molar masses of CHO/CPO copolymers.

CPO (mol%)	CPO (wt%)	T_g (K)	T_g (°C)	$T_{g,Fox}$ (K)[a]	ΔT_g (K)[b]	M_n (kg mol^{-1})
0	0.0	337.3	64.2	337.3	–	19
3	2.6	325.6	52.5	334.5	−8.9	18.5

CPO (mol%)	CPO (wt%)	T_g (K)	T_g (°C)	$T_{g,Fox}$ (K)[a]	ΔT_g (K)[b]	M_n (kg mol^{-1})
5.4	4.7	313.8	40.7	332.3	−18.5	20.3
10.3	9.0	311.0	37.9	327.8	−16.8	18
19.4	17.1	308.6	35.5	319.6	−11.0	16.6
27	24.1	305.7	32.6	312.9	−7.2	17.7
35	31.6	302.7	29.6	306.1	−3.4	16
46.3	42.5	294.3	21.2	296.6	−2.3	18.5
62.5	58.8	282.2	9.1	283.4	−1.2	18.6
76.9	74.0	271.3	−1.8	272.2	−0.9	18.6
85.2	83.1	264.8	−8.3	265.8	−1.0	19.2
100	100.0	254.9	−18.3	254.9	–	20

[a] Calculated with the Fox equation, $1/T_g = w_1/T_{g1} + w_2/T_{g2}$, from the homopolymer values and the weight fractions (repeat-unit molar masses 98.14 and 84.12 g mol^{-1}). [b] $\Delta T_g = T_g - T_{g,Fox}$.

Fig. 4 shows a pronounced negative deviation of T_g from both linear additivity and the Fox equation. The deviation is concentrated at low CPO contents. Incorporation of only 3 mol% CPO lowered T_g by 11.7 K, and 5.4 mol% CPO lowered it by 23.5 K, which is 18.5 K below the Fox prediction. Between about 5 and 35 mol% CPO, T_g decreased only slowly (from 313.8 to 302.7 K). Above about 40 mol% CPO, the experimental values approached the Fox curve to within 1–2 K.

Because the CHO and CPO repeat units differ only in the size of the pendant cycloalkane ring, the 82 K difference between the homopolymer T_g values must reflect the restriction that the ring imposes on rotation about the C–C and C–O bonds of the polyether backbone. The cyclopentane ring is smaller than the cyclohexane ring and is conformationally more flexible, so it hinders backbone rotation less. In CHO-rich copolymers, the sequence analysis above shows that each CPO unit is isolated between CHO units. A small cyclopentane ring between two cyclohexane rings relieves the steric interaction between neighbouring cyclohexane rings and allows easier rotation of the adjacent backbone bonds and of the flanking cyclohexane rings themselves. Each CPO unit therefore mobilizes not only its own segment but also those of its neighbours. This explains the disproportionate effect of the first few mole percent of CPO on T_g.

This interpretation implies that the influence of a CPO unit extends beyond the nearest-neighbour dyads. A Johnston-type dyad analysis [13], using the terminal-model dyad probabilities calculated from the NLLS reactivity ratios and a single adjustable heterodyad T_g (best fit 277 ± 8 K), described the data above about 20 mol% CPO to within about 6 K but underestimated the decrease at 3–10 mol% CPO by 8–17 K. A dyad model can therefore not account for the steep initial decrease, which is consistent with the longer-range mobilizing effect proposed above.

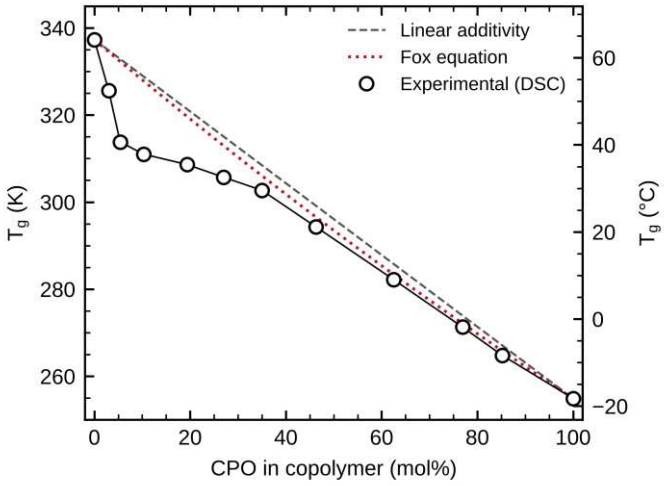


Fig. 4 Glass transition temperature of CHO/CPO copolymers as a function of CPO content (Table 4). The dashed line represents linear additivity between the homopolymer values and the dotted curve the Fox equation

3.4. ^{13}C NMR spectra of the homopolymers

The ^{13}C NMR spectra of the two homopolymers are strikingly different (Fig. 5). Poly(CPO) gives three sharp, well-resolved resonances: the backbone methine carbons (CH–O) at δ 83.4 and 83.6 ppm, and the ring methylene carbons at δ ≈ 30.5 ppm (C-3/C-5) and δ ≈ 21.4 ppm (C-4). In poly(CHO), the methylene carbons give broad multiplets centred at δ ≈ 29 and δ ≈ 23 ppm, and the methine signal (δ ≈ 78 ppm) appears as a broad multiplet partly overlapped by the $CDCl_3$ triplet.

We attribute the sharp lines of poly(CPO) to the conformational freedom of the pendant cyclopentane rings, which rotate and pseudorotate rapidly about the polymer backbone, so that each carbon gives a single time-averaged resonance. The larger cyclohexane rings of poly(CHO) are more hindered. In addition, they can interconvert between chair and twist-boat conformations, which generates a range of local environments for the ring carbons and broadens the signals. Sensitivity of the ring carbons to the configurational sequence (diad and triad stereosequences of the (*R*,*R*) and (*S*,*S*) units formed by *trans* ring opening) may also contribute to the multiplet structure [16]. Either way, the NMR line shapes are consistent with the greater segmental mobility of CPO units deduced from the T_g data.

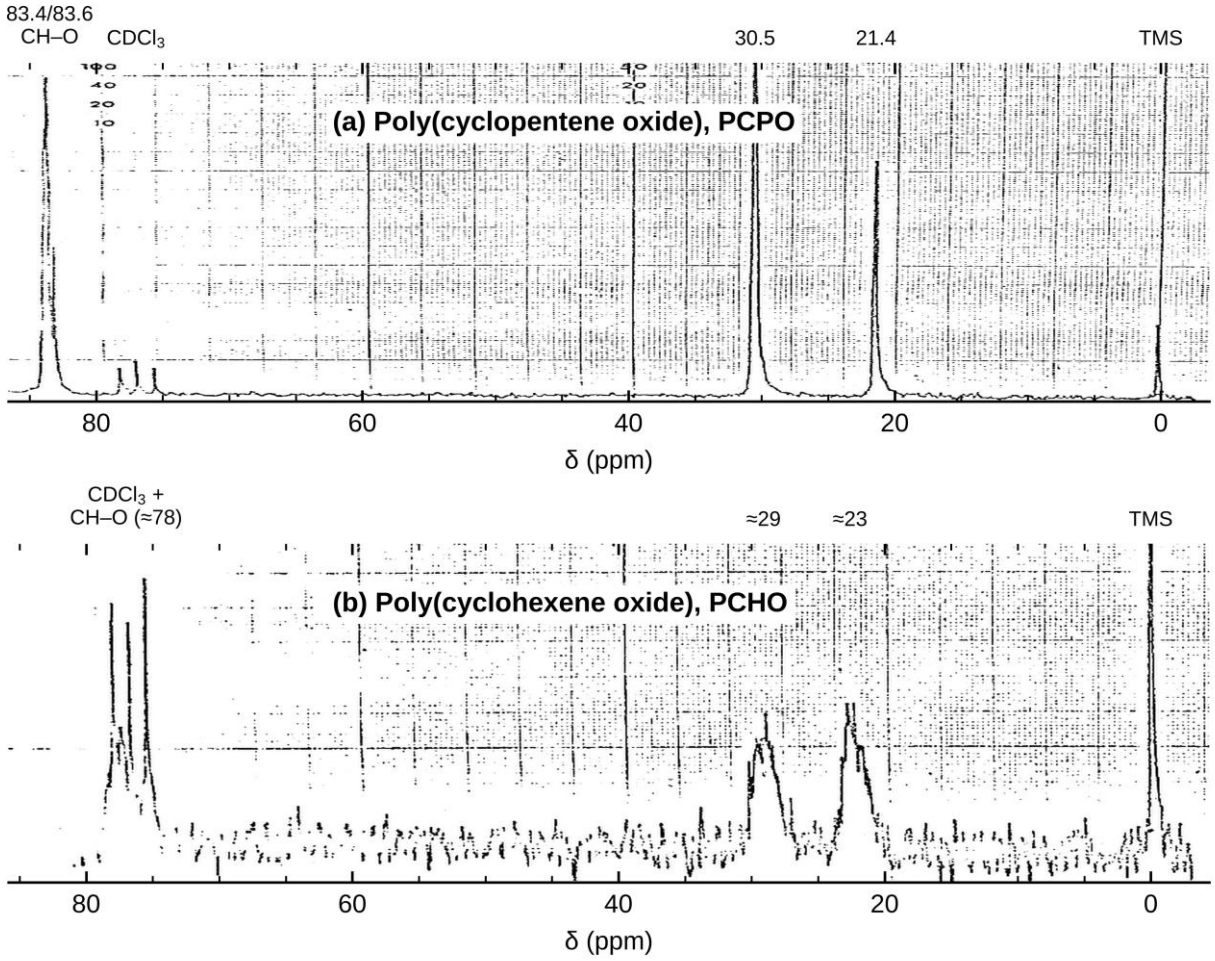


Fig. 5 ^{13}C NMR spectra (25.2 MHz, $CDCl_3$, TMS) of (a) poly(cyclopentene oxide) and (b) poly(cyclohexene oxide). Chemical shifts are referenced to TMS (δ 0) and the $CDCl_3$ triplet (δ 77.0)

3.5. Scope of the data

Some limitations of the data should be noted. The ^{13}C NMR spectra were recorded at 25.2 MHz with broadband ^{1}H decoupling, so nuclear Overhauser effects may introduce small systematic errors in the integrated compositions. The close agreement of all ten compositions with the terminal model (root-mean-square residual 0.016 in F_{CHO}) and the consistency of the linear and nonlinear estimates indicate that such errors are small compared with the composition effects discussed here. Molar-mass dispersities were not determined, and each T_g value derives from a single DSC measurement. The steep decrease of T_g at low CPO contents is, however, defined by three consecutive compositions (3.0, 5.4 and 10.3 mol% CPO) and is not accompanied by any change in M_n. Further measurements in the 0–10 mol% CPO range with modern high-field NMR and replicate DSC would refine, but are not expected to alter, the conclusions drawn here.

4. Conclusions

Cyclohexene oxide and cyclopentene oxide undergo photoinitiated cationic copolymerization with PTPDS PF_6^- over the entire feed range to give statistical copolymers with a single T_g. CHO is the more reactive monomer in both homopolymerization (R_p ratio 1.8) and copolymerization. Nonlinear least-squares analysis gave r_{CHO} = 2.65 ± 0.25 and r_{CPO} = 0.77 ± 0.08, in good agreement with the Kelen–Tüdős values of 2.45 and 0.69. The 95% joint confidence region excludes ideal copolymerization. The T_g decreases from 337.3 to 254.9 K across the composition range, with a strong negative deviation from the Fox equation at low CPO contents, while M_n is independent of composition. Small amounts of CPO therefore provide an efficient way to lower the T_g of CHO-based cationically cured networks and to increase their flexibility without changing the molar mass. This is a useful design parameter for cycloaliphatic epoxide coating and adhesive formulations.

Acknowledgements

Support of this work by the University of Petra is gratefully acknowledged.

Statements and Declarations

Funding This work has no funding source

Competing interests The authors have no relevant financial or non-financial interests to disclose.

Author contributions Conceptualization, investigation and writing – original draft: I.I. Abu-Abdoun; formal analysis: A.M. Al Tweiq; data curation: L.N. Ali. All authors read and approved the final manuscript.

Data availability All data generated or analysed during this study are included in this published article.

Ethics approval Not applicable.

References

1. Crivello JV, Lam JHW (1977) Diaryliodonium salts. A new class of photoinitiators for cationic polymerization. Macromolecules 10:1307–1315. https://doi.org/10.1021/ma60060a028

2. Crivello JV, Lam JHW (1979) Photoinitiated cationic polymerization with triarylsulfonium salts. J Polym Sci Polym Chem Ed 17:977–999. https://doi.org/10.1002/pol.1979.170170405

3. Crivello JV (1999) The discovery and development of onium salt cationic photoinitiators. J Polym Sci A Polym Chem 37:4241–4254. https://doi.org/10.1002/(SICI)1099-0518(19991201)37:23<4241::AID-POLA1>3.0.CO;2-R

4. Sangermano M, Razza N, Crivello JV (2014) Cationic UV-curing: technology and applications. Macromol Mater Eng 299:775–793. https://doi.org/10.1002/mame.201300349

5. Crivello JV, Varlemann U (1995) Mechanistic study of the reactivity of 3,4-epoxycyclohexylmethyl 3′,4′-epoxycyclohexanecarboxylate in photoinitiated cationic polymerizations. J Polym Sci A Polym Chem 33:2473–2486. https://doi.org/10.1002/pola.1995.080331421

6. Mayo FR, Lewis FM (1944) Copolymerization. I. A basis for comparing the behavior of monomers in copolymerization; the copolymerization of styrene and methyl methacrylate. J Am Chem Soc 66:1594–1601. https://doi.org/10.1021/ja01237a052

7. Fineman M, Ross SD (1950) Linear method for determining monomer reactivity ratios in copolymerization. J Polym Sci 5:259–262. https://doi.org/10.1002/pol.1950.120050210

8. Kelen T, Tüdős F (1975) Analysis of the linear methods for determining copolymerization reactivity ratios. I. A new improved linear graphic method. J Macromol Sci A Chem 9:1–27. https://doi.org/10.1080/00222337508068644

9. Tidwell PW, Mortimer GA (1965) An improved method of calculating copolymerization reactivity ratios. J Polym Sci A 3:369–387. https://doi.org/10.1002/pol.1965.100030137

10. Autzen AAA, Beuermann S, Drache M, Fellows CM, Harrisson S, van Herk AM, Hutchinson RA, Kajiwara A, Keddie DJ, Klumperman B, Russell GT (2024) IUPAC recommended experimental methods and data evaluation procedures for the determination of radical copolymerization reactivity ratios from composition data. Polym Chem 15:1851–1861. https://doi.org/10.1039/D4PY00270A

11. Fox TG (1956) Influence of diluent and of copolymer composition on the glass temperature of a polymer system. Bull Am Phys Soc 1:123

12. Gordon M, Taylor JS (1952) Ideal copolymers and the second-order transitions of synthetic rubbers. I. Non-crystalline copolymers. J Appl Chem 2:493–500. https://doi.org/10.1002/jctb.5010020901

13. Johnston NW (1976) Sequence distribution–glass transition effects. J Macromol Sci Rev Macromol Chem C14:215–250. https://doi.org/10.1080/15321797608065770

14. Barton JM (1970) Relation of glass transition temperature to molecular structure of addition copolymers. J Polym Sci C 30:573–597. https://doi.org/10.1002/polc.5070300161

15. Abu-Abdoun II, Aal-e-Ali A (1993) Photopolymerization of cyclohexene oxide by phosphonium and arsonium salts. Eur Polym J 29:1445–1450. https://doi.org/10.1016/0014-3057(93)90056-L

16. Abu-Abdoun II (1999) Photo-initiated polymerization of cyclohexene oxide by dirhenium decacarbonyl. Polym Int 48:1197–1201. https://doi.org/10.1002/(SICI)1097-0126(199912)48:12<1197::AID-PI284>3.0.CO;2-A

17. Smith GH (1979) US Patent 4,173,476

18. Abu-Abdoun II (2021) Synthesis and applications of polymeric reagent p-substituted triphenylamine. J Res Updates Polym Sci 10:51–57. https://doi.org/10.6000/1929-5995.2021.10.7

19. Odian G (2004) Principles of polymerization, 4th edn. Wiley-Interscience, Hoboken